International Journal of the Korean Society of Precision Engineering, Vol. 2, No. 3, September 2001.

Analysis on Short Crack Growth Rate after Single Overload under Cyclic Bending Moment

Sam-Hong Song[1], Kyeong-Ro Lee[2] and Amkee Kim[3]

[1] Department of Mechanical Engineering, Korea University, Seoul, Korea
[2] Division of Machinery & Automobiles, Shinsung College, Chungnam, Korea
[3] Department of Mechanical Engineering, Kongju National University, Chungnam, Korea

ABSTRACT

In order to investigate the effect of single tensile overload on the short crack growth behavior under the out-of-plane cyclic bending moment, crack opening stresses were continuously measured by an elastic compliance method using strain gages. The characteristics of short crack growth after the single tensile overload are analyzed by the effective stress range ratio. Futhermore, the investigation was carried out with respect to various fatigue crack growth behaviors such as the plastic zone size effect on crack retardation, the retarded crack length and the number of cycles.

Keywords: Short Crack, Fatigue Crack Growth, Overload, Stress Intensity Factor Range, Crack Opening Stress, Effective Stress Range Ratio

1. Introduction

The study on fatigue life under variable loading has been an important subject in predicting the fatigue life of structures or machinery components.[1-3] Particularly, the study on the fatigue crack growth behavior after a single tensile overload has been attempted since it might provide a fundamental theory regarding the fatigue life under variable loading. As far as the single overloading effects on the fatigue crack growth rate are concerned, previous studies have revealed the occurrence of retardation after the overload,[4-7] or the retardation preceded by the acceleration in a short distance after the overload. Which way the crack should go depends on the loading condition and the mode of crack.[8] However, since those behaviors are characterized by the experimental observations of long through thickness crack because of experimental difficulties, the obscurity of the short crack growth behavior after the overload still remains.

The growth rate of short crack under the constant amplitude cyclic loading is known to be faster than that of the long crack under the same range of stress intensity factor, ΔK. The discrepancy was often resolved by employing the effective stress intensity factor, ΔK_{eff}, taking into account the crack closure. Therefore the analysis on the short crack growth behavior after the overload based on the crack closure might provide beneficial informations for the fatigue life prediction.

In this research, the fatigue crack growth test of short crack was performed under cyclic bending moment as well as the long crack for the comparison. The crack opening stresses were measured by an elastic compliance method using strain gages, which can continuously collect data during the cyclic loading. The characteristics of short crack growth rate after the single tensile overload are analyzed by the effective stress range ratio. The investigation was also carried out on various relationships among the plastic zone size, the retardation crack length, the number of retardation cycles so on.

2. Experimental

2.1 Material and specimen

The test material is Cr-Mo alloy steel, SA-387, that

Table 1 Mechanical properties of the test material

Yield strength (MPa)	Ultimate tensile strength (MPa)	Elongation (%)	Elasticity modulus (MPa)	Poisson's ratio
350	585	24	191200	0.28

is widely used as a pressure vessel material in the industry. The mechanical properties are contained in Table 1. The geometry of specimen for the bending fatigue test is depicted in Fig. 1. The crack length, a, is defined as the half of total crack length including a hole with 0.5mm in diameter and 0.5mm in depth on the specimen surface. The fatigue crack initiates and grows from the hole. The crack length was measured by a travelling microscope while stopping the test machine. The 140 times magnification for the measurement of long crack and the 280 times magnification for the measurement of short crack were utilized respectively.

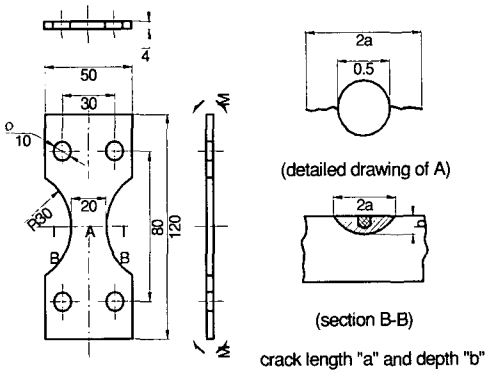

Fig. 1 Geometries of bending fatigue test specimen

2.2 Experimental setup and method

Fig. 2 represents a fatigue stress model on the specimen surface applied by the cyclic out-of-plane bending moment, where the regular fatigue stress ratio $R=-1$. Since the many components of machinery are exposed to the cyclic bending moment, this study focuses on the crack growth behavior under cyclic bending moment. The single overload stress twice higher than the regular maximum fatigue stress(167 MPa) was applied. The effects of the single overload on the short and long crack growth were represented in terms of crack

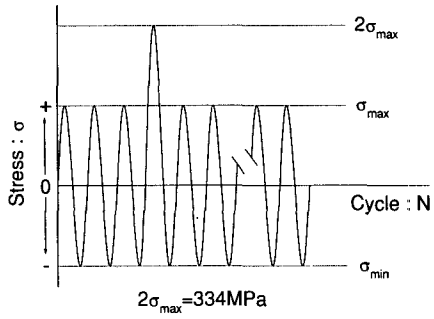

Fig. 2 Schematic representation of fatigue stress model

growth rate.

Measurement methods for the crack opening stress due to crack closure are categorized into the direct measurement method and the indirect measurement method. The SEM method, the replica method and the laser interferometric strain/displacement gage method belong to the direct measurement method. On the other hand, the clip gage, strain gage method[9] and ultrasonic method belong to the indirect measurement method. Since the direct measurement method is time consuming and difficult to obtain data enough to analyse, the indirect methods such as strain gage method are preferably used. In this study, an elastic compliance method using two 120Ω strain gages was employed for measuring the crack opening stresses. One(1.0mm gage) is located 20mm away from the hole, and the other(0.3mm gage) is attached next to the hole. Fig. 3 depicts the locations of strain gages in the specimen. 1.0mm gage and 0.3mm gage measure the nominal strain produced by the external bending moment and the local strain close to the crack tip respectively, which allows for the estimation of crack opening and closing points.

The variation of resistance of strain gage is converted to the variation of voltage by an electrical bridge circuit. After the amplification of voltage, the analog signals from two strain gages are digitized by A/D converters. The data are analyzed by the computer for determining the opening stress range ratio. All devices were grounded in order to prevent the electrical noise. The frequency of cyclic loading was 33Hz, and over 200 data per cycle from both strain gages were analyzed. Details of technique regarding the determination of crack opening and closing

points are described in the references.[9,10]

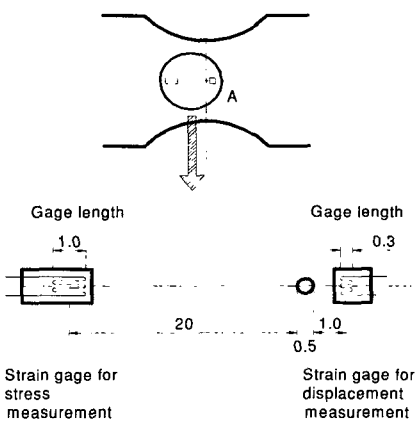

Fig. 3 Strain gages on the specimen (unit: mm)

3. Results and Discussion

3.1 Crack growth behaviors under the constant amplitude cyclic moment

Fig. 4 represents the relationship between crack growth rate, da/dN, and crack length, a, under the constant amplitude cyclic moment without the overload. The non-monotonous peculiar behavior of crack growth up to 0.65mm is manifest. Thus, terminologies, "short" and "long", to distinguish between the cracks shorter and longer than 0.65mm were used in this study.

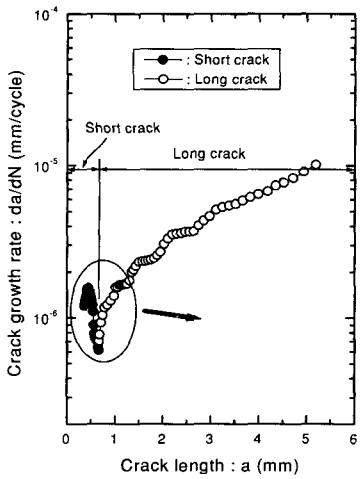

Fig. 4 Relation between crack growth rate and crack length at $R=-1$, $\sigma_{max}=167$MPa

Fig. 5 represents the relationship between the stress intensity factor range, ΔK, and the crack growth rate, da/dN, in three different cases; the short crack under the constant cyclic bending moment, the long crack under the constant cyclic bending moment and the long crack under the ASTM test. The stress intensity factors of crack under the cyclic bending moment were evaluated by Newman's equation in ASTM-E740.[11] The crack growth rate data based on ASTM-E647[12] are also represented in the figure.

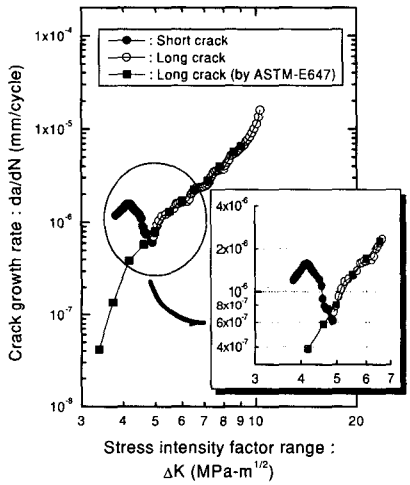

Fig. 5 Relation between crack growth rate and stress intensity factor range for short crack and long crack at $R=-1$

The peculiar growth rate behavior of short crack in Fig. 4 also appears in Fig. 5 using ΔK in contrast with the monotonous behavior from the standard test of long crack. It indicates that the short crack growth might be affected by the microstructure such as inclusion, grain boundary and the residual plastic deformation formed along the wake of crack. Moreover, the growth of crack initiated from the notch(hole) seems to be affected by the stress field around the notch rather than the stress intensity of crack. Thus the crack growth rate of the short crack could be faster than that of the long crack even at the same ΔK. On the other hand, since the precision machinery is malfunctioned by the mismatch of components due to the small deformation or the short crack, it is important for one to understand the effect

of overload on short crack growth. However, most of previous researches regarding the overload effect are focused on the long crack rather than the short crack mainly due to experimental difficulties.

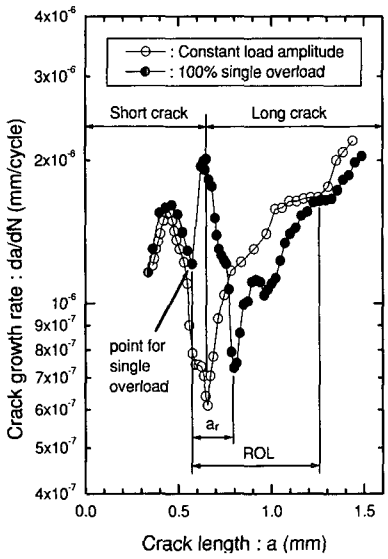

Fig. 6 Comparison between crack growth rates with and without the single overload at $a=0.58$mm

3.2 Crack growth behavior after the single overload

In this study, a single overload was applied at $a=0.58$mm for the short crack, at $a=1.61$mm for the long crack and at $a=3.20$mm for the enough long crack, respectively.

Fig. 6 represents curves of da/dN versus a with a single overload at $a=0.58$mm(short crack). The crack growth rate after the overload increases and decreases rapidly within the short distance. After the local minimum point of crack growth rate in the figure, the relatively long retardation region appears where the crack growth rate is lower than that without the overload. Even in the region where crack growth rate decreases drastically under the constant cyclic moment without the overload(the transition region from the short crack to the long crack; $a=0.45\sim0.65$mm), the crack growth rate after the overload increases drastically. In this study, the region where the crack growth behavior is affected by the overload is designated as *ROL*, and the distance

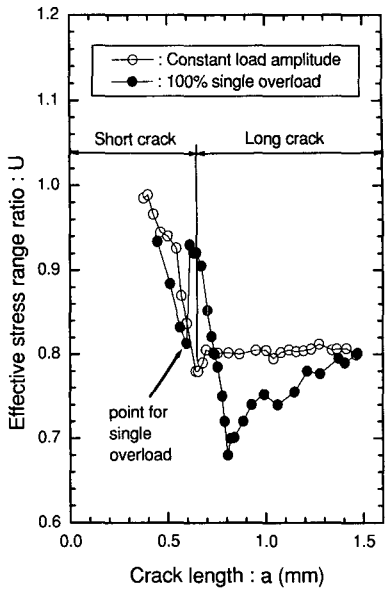

Fig. 7 Comparison between effective stress range ratios with and without the overload at $a=0.58$mm

from the point of overload to the point at which the crack growth rate is minimum is designated as a_r.

Fig. 7 represents the relation between the effective stress range ratio, U, and the crack length, a. The effective stress range ratio, U, was calculated by equation (1).

$$U = \frac{\Delta K_{eff}}{\Delta K} = \frac{\sigma_{max} - \sigma_{op}}{\sigma_{max}} \quad (1)$$

ΔK_{eff} : effective stress intensity factor range
σ_{max} : maximum stress by cyclic moment
σ_{op} : crack opening stress

Fig. 7 indicates that the effective crack stress ratio, U, increases drastically after the overload as the crack growth rate increases in the range of $a=0.58\sim0.65$mm. And U decreases as the crack growth rate decreases in the range of $a=0.65\sim0.79$mm. In other words, the pattern of U variation after the overload is very similar to that in Fig. 6. As results, the effective stress range ratio, U, might provide a clue for the analysis of crack growth behavior after the overload.

Fig. 8 represents curves of da/dN versus a with

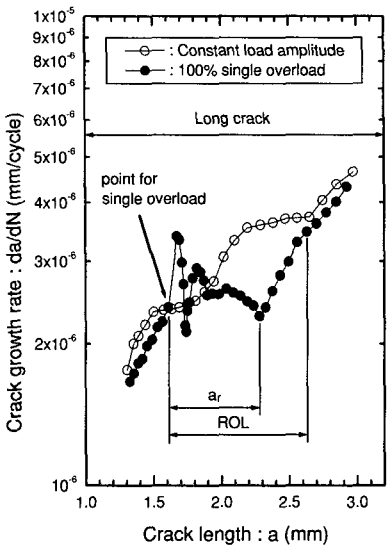

Fig. 8 Comparison between crack growth rates with and whthout the single overload at $a = 1.61$ mm

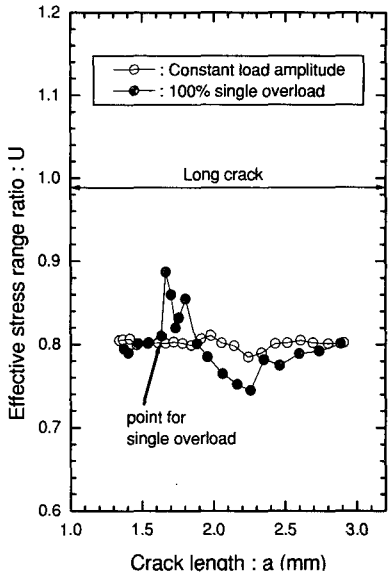

Fig. 9 Comparison between effective stress range ratios with and without the single overload at $a = 1.61$mm

a single overload at $a = 1.61$mm(long crack). Fig. 9 shows the relationship between the effective stress range ratio, U, and the crack length, a, with a single overload at $a = 1.61$mm.

The crack growth rate, da/dN, and the effective stress ratio, U, after the overload at $a = 3.20$mm(enough long crack) are compared with those under the constant amplitude cyclic moment without the overload in Fig. 10 and Fig. 11, respectively. Here, the crack growth rate just after the overload is drastically accelerated and decelerated again. The retardation range appears within the comparatively long range. After that, the retardation finally disappears. Considering Fig. 9 and Fig. 11, the crack growth rate behavior after the overload well coincides with the variation of U in case of Fig. 7. The abrupt increasement and the subsequent decrease of effective stress range ratio after the overload is in good agreement with the results by the three dimensional elasto-plastic finite element analysis of crack closure and opening under cyclic loading with a single overload.[13]

Several mechanisms of crack growth after the overload have been proposed to rationalize experimental results as follows[14]: (1) residual stress, (2) crack closure, (3) plastic blunting, (4) crack deflection, (5) strain hardening. In fact, those are correlated with each other except for the crack deflection. For that reason, the models to predict fatigue crack growth rate used to be based on crack closure.[12] The residual deformation exists along the wake zone of fatigue crack provided by the previous load history, which allows the crack to close even under the tensile stress. Thus the sudden increase of crack growth rate after the overload and the subsequent crack retardation in this study could be qualitatively explained by U.

3.3 Relationship between plastic zone size and crack growth rate

The plastic zone size, ω_{ol}, by the overload can be calculated as follows.[15]

$$\omega_{ol} = \frac{4K^2}{\pi\beta\sigma_y^2} \tag{2}$$

Where β is 1 in case of plane stress state, and 3 in case of plane strain state. Since the crack length was measured on the surface of specimen in this study, β was taken as 1. Fig. 12 indicates that a_i is the crack length at the overload and a_j is the crack length after which the overload does not have influence on the crack

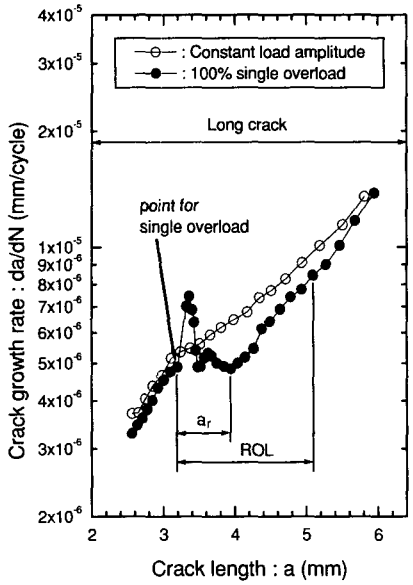

Fig. 10 Comparison between crack propagation rates with and without the single overload at $a=3.20$mm

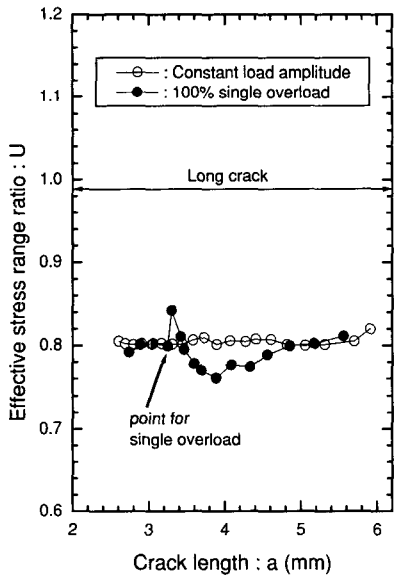

Fig. 11 Comparison between effective stress range ratios with and without the single overload at $a=3.20$mm

growth rate. If the number of cycles retarded(or promoted) by the overload, N_d, is defined by equation (3).

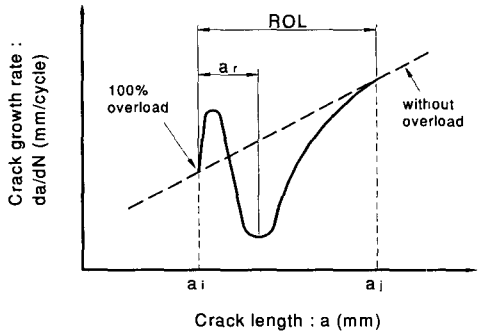

Fig. 12 Schematic illustration to calculate retarded (or promoted) cycles and distances after the overload

$$N_d = (N_{aj}-N_{ai})_{ol} - (N_{aj}-N_{ai})_{cl} \qquad (3)$$

Here, N_{ai} is the number of cycles to a_i. N_{aj} is the number of cycles to a_j. $(N_{aj}-N_{ai})_{ol}$ is the difference between N_{ai} and N_{aj} due to the overload. And $(N_{aj}-N_{ai})_{cl}$ is the difference between N_{ai} and N_{aj} without the overload.

The retarded(or promoted) crack length, a_d, is calculated by equation (4).

$$a_d = N_d \times \left(\frac{da}{dN}\right)_m \qquad (4)$$

where a mean value of crack growth rate between a_i and a_j, $\left(\frac{da}{dN}\right)_m$, can be calculated by equation (5).

$$\left(\frac{da}{dN}\right)_m = \frac{a_j-a_i}{(N_{aj}-N_{ai})_{cl}} \qquad (5)$$

Table 2 contains the characteristics of a_r, ω_{ol}, N_d, a_d and N_d/N_f in cases of overload at three different crack lengths, 0.58mm, 1.61mm and 3.20mm. $OL1$, $OL2$ and $OL3$ are corresponding to crack lengths at overload, 0.58mm, 1.61mm and 3.20mm respectively. It is recognized from all cases that a_r coincides with plastic zone size, ω_{ol}. The size of ROL(range affected by overload) in case of $OL1$(short crack) is 3 times bigger than ω_{ol}. On the other hand, those in case of $OL2$(long crack) and $OL3$(enough long crack) are about twice. Particularly, in case of $OL1$, the overall crack growth

rate is higher(promoted) than that without the overload in comparison with the retardation in cases of *OL2* and *OL3*. The number of cycles due to the influence of overload appears small, less than 3% of the entire fatigue life, in all cases.

Table 2 Various phenomena after 100% single overload

	OL1 (0.58mm)	*OL2* (1.61mm)	*OL3* (3.20mm)
ROL(mm)	0.68	1.02	1.58
a_r (mm)	0.23	0.67	0.75
ω_{ol} (mm)	0.23	0.50	0.78
N_d (cycle)	Promotion 2.18×10^4	Retardation 5.60×10^4	Retardation 3.79×10^4
a_d (mm)	Promotion 0.03	Retardation 0.18	Retardation 0.25
N_d/N_f (%)	Promotion 1.14	Retardation 2.93	Retardation 1.98
Fatigue life of constant load amplitude $N_f = 1.91\times10^6$ cycle			

4. Conclusion

In order to observe the effect of single tensile overload on the behaviors of short crack under out-of-plane bending fatigue, the crack opening stress after the single overload were measured by an elastic compliance method using strain gages. The relationship between crack growth behaviors and effective stress range ratio was investigated. The plastic zone size formed at the crack tip and the retarded(or promoted) crack length and the number of retarded(or promoted) cycles were also investigated. The results are as follows.

1. The crack behavior after the overload shows that the crack growth rate increases, decreases rapidly, and finally approaches to the crack growth rate without overload. This phenomenon is common in both short crack and long crack, and can be qualitatively explained by the effective stress range based on the crack closure.

2. The location where the maximum retarded crack growth rate occurs after the overload well coincides with the plastic zone size formed by the overload. The range affected by the single overload is more than twice bigger than the size of the plastic zone.

3. Retardation effect(especially in tensile-tensile test) after the overload is reduced by the acceleration immediately after the overload under bending load. Especially, the effect of acceleration is more pronounce in the short crack.

References

1. Cho, S. S., Jang, D. Y., and Joo, W. S., "A Study on the Prediction of Fatigue Damage in 2024-T3 Aluminum Alloy Using Neural Networks," Journal of Korean Society of Precision Engineering, Vol. 16, No. 7, pp. 168-177, 1999.
2. Cho, S. S., Kim, S. H., and Joo, W. S., "A Study on the Prediction of Fatigue Life in 2024-T3 Aluminum Using X-ray Half-value Breadth," Journal of Korean Society of Precision Engineering, Vol. 17, No. 1, pp. 145-152, 2000.
3. Song, S. H., Bae, J. S., and Choi, B. H., "An Experimental Study on the Fatigue Behavior and Stress Interaction of Arbitrarily Located Defects(II) (For Variable Loads and Distances between Defects)," Journal of Korean Society of Precision Engineering, Vol. 18, No. 1, pp. 201-212, 2001.
4. Gan, D., and Weertman, J., "Fatigue Crack Closure after Overload," Engineering Fracture Mechanics Vol. 18, No. 1, pp. 155-160, 1983.
5. Kurihara, M., Katoh, A., and Kawahara, M., "Effects of Stress Ratio and Step Loading on Fatigue Crack Propagation Rate," Current Research on Fatigue Cracks, Current Japanese Materials Research, Vol. 1, pp. 247-265, 1987.
6. Schijve, J., "Some Formulas for the Crack Opening Stress Level," Engineering Fracture Mechanics, Vol. 14, pp. 461-465, 1981.
7. Pantelakis, Sp. G., Kermanidis, Th. B., and Pavlou, D.G., "Fatigue Crack Growth Retardation Assessment of 2024-T3 and 6061-T6 alumininum specimens," Theoretical and Applied Fracture Mechanics, Vol. 22, pp. 35-42, 1995.
8. Song, S. H., and Won, S. T., "Behavior of Initiation and Propagation of Fatigue Crack under Periodic Overstressing (I)," Transactions of the KSME, Vol.

9, No. 3, pp. 301-308, 1985.

9. Elber, W., "The Significance of Fatigue Crack Closure," Damage Tolerance in Aircraft Structures, ASTM STP 468, pp. 230-242, 1971.
10. Park, J. H., Song, J. H., Earmme, Y. Y., Kim, C. Y., and Kang, K., J., "Personal Computer-Based Fatigue Testing Automation and Improvement in Fatigue Behavior Monitoring," Transactions of the KSME, Vol. 12, No. 1, pp. 123-130, 1988.
11. "Standard Practice for Fracture Testing With Surface-Crack Tension Specimens," Annual Books of ASTM Standards, Vol. 03.01, E740-88, pp. 689-696, 1988.
12. "Standard Test Method for Measurement of Fatigue Crack Growth Rates," Annual Books of ASTM Standards, Vol. 03.1, E647-91, pp. 674-701, 1991.
13. Chermahini, R. G., Shivanumar, K. N., and Newman, J. C. Jr., "Three-Dimensional Finite-Element Simulation of Fatigue Crack Growth and Closure," Mechanics of Fatigue Crack Closure, ASTM STP 982, pp. 398-413, 1988.
14. Ward-Close, C. M., and Ritchie, R. O., "On the Role of Crack Closure Mechanisms in Influencing Fatigue Crack Growth Following Tensile Overloads in a Titanium Alloy : Near Threshold Versus Higher ΔK Behavior," Mechanics of Fatigue Crack Closure, ASTM STP 982, pp. 93-111, 1988.
15. Anderson, T. L., Fracture Mechanics Fundamentals and Applications, CRC Press, Boston, pp. 620-629, 1991.